Computers and Mathematics with Applications 77 (2019) 2894–2905

Contents lists available at ScienceDirect

Computers and Mathematics with Applications

journal homepage: www.elsevier.com/locate/camwa

On numerical approximation of a variational–hemivariational inequality modeling contact problems for locking materials

Mikaël Barboteu [a], Weimin Han [b,*], Stanisław Migórski [c]

[a] Laboratoire de Mathématiques et PhySique (LAMPS), Université de Perpignan, 52 Avenue Paul Alduy, 66860 Perpignan, France
[b] Program in Applied Mathematical and Computational Sciences (AMCS) and Department of Mathematics, University of Iowa, Iowa City, IA 52242, USA
[c] Jagiellonian University in Kraków, Chair of Optimization and Control, ul. Łojasiewicza 6, 30348, Kraków, Poland

A R T I C L E I N F O

Article history:
Available online 23 August 2018

Dedicated to Professor Mircea Sofonea on the occasion of his 60th birthday

Keywords:
Variational–hemivariational inequality
Locking material
Unilateral constraint
Nonmonotone friction
Finite element method
Error estimate

A B S T R A C T

This paper is devoted to numerical analysis of a new class of elliptic variational–hemivariational inequalities in the study of a family of contact problems for elastic ideally locking materials. The contact is described by the Signorini unilateral contact condition and the friction is modeled by a nonmonotone multivalued subdifferential relation allowing slip dependence. The problem involves a nonlinear elasticity operator, the subdifferential of the indicator function of a convex set for the locking constraints and a nonconvex locally Lipschitz friction potential. Solution existence and uniqueness result on the inequality can be found in Migórski and Ogorzaly (2017) . In this paper, we introduce and analyze a finite element method to solve the variational–hemivariational inequality. We derive a Céa type inequality that serves as a starting point of error estimation. Numerical results are reported, showing the performance of the numerical method.

1. Introduction

Variational–hemivariational inequalities are a particular kind of inequality problems, in which both convex and nonconvex functions are involved. Motivated by applications in contact mechanics, several variational–hemivariational inequalities have been studied recently. In [1], a class of static variational–hemivariational inequalities is introduced and well-posedness of the inequalities is shown. The finite element method is applied for the numerical approximation and error estimates are derived. For the linear element solutions, the optimal convergence order is shown under certain solution regularity assumptions. This represents the first optimal order error bound found in the literature on numerical solutions of hemivariational inequalities or variational–hemivariational inequalities. The results are applied in the analysis of static contact problem with friction for elastic materials. In [2], a viscoelastic problem is considered on infinite time interval, modeled with frictionless contact and with a boundary condition which describes both the instantaneous and the memory effects of the foundation. This problem leads to a variational–hemivariational inequality with history-dependent operators. In [3], a class of elliptic variational–hemivariational inequalities is studied in reflexive Banach spaces. Well-posedness of the inequalities is established, including a result on the continuous dependence of the solution with respect to the data and a convergence result obtained by means of penalization method. The abstract results are applied to the study of an elastic contact problem with unilateral constraint. Numerical analysis of the problems studied in [3] is done in [4], where a general framework of convergence and error estimation is established.

* Corresponding author.
E-mail addresses: barboteu@univ-perp.fr (M. Barboteu), weimin-han@uiowa.edu (W. Han), stanislaw.migorski@uj.edu.pl (S. Migórski).

https://doi.org/10.1016/j.camwa.2018.08.004
0898-1221/

In the very recent paper [5], new variational–hemivariational inequalities are introduced and analyzed for static contact problems for elastic ideally locking materials. The contact is assumed to be static and it is modeled by the Signorini unilateral contact condition with a nonmonotone friction condition between a locking body and a rigid foundation. The constitutive law is described by the (convex) subdifferential of the indicator function of a convex set which characterizes the locking constraints. The friction is modeled by the (Clarke) subdifferential boundary condition involving a locally Lipschitz function which is generally nonconvex and nondifferentiable. Furthermore, the multivalued frictional contact condition is allowed to depend on the slip, important for many applications. The weak formulation has a form of variational–hemivariational inequality of elliptic type. This appears to be the first work on variational–hemivariational inequalities for locking materials.

The theory of locking materials started with the pioneering works by Prager, [6–8]. Here, locking materials refer to hyperelastic bodies with the strain tensor constrained to a convex set. We use a positive integer d for the spatial dimension; for applications, $d \le 3$. Let $\mathbb{S}^d$ be the space of second order symmetric tensors on $\mathbb{R}^d$, and B be a closed, convex subset of $\mathbb{S}^d$ with $\mathbf{0}_{\mathbb{S}^d} \in B$. The elastic ideally locking materials are characterized by the following relations

$$\begin{cases} \sigma_{ij} = \sigma^e_{ij} + \sigma^l_{ij}, \quad \sigma^e_{ij} = a_{ijkl}\varepsilon_{kl}(\boldsymbol{u}), \\ \boldsymbol{\varepsilon}(\boldsymbol{u}) \in B, \quad \sigma^l_{ij}\cdot(\varepsilon^*_{ij} - \varepsilon_{ij}(\boldsymbol{u})) \le 0 \ \text{ for all } \boldsymbol{\varepsilon}^* = (\varepsilon^*_{ij}) \in B. \end{cases} \tag{1}$$

Here σ^e_{ij} and σ^l_{ij} represent elastic and locking components of the stress tensor σ_{ij}, $\boldsymbol{u}$ is the displacement field, and $\boldsymbol{\varepsilon}(\boldsymbol{u}) = (\varepsilon_{ij}(\boldsymbol{u}))$ is the infinitesimal strain tensor with the components $\varepsilon_{ij}(\boldsymbol{u}) = \frac{1}{2}(u_{i,j} + u_{j,i})$. The indices i, j, k, l run between 1 and d, and the summation convention over repeated indices is adopted. As an example of one spatial dimension, a stress–strain law of the type (1) takes the form [6]

$$\sigma = \begin{cases} 0, & \text{if } \varepsilon < 0, \\ k\varepsilon, & \text{if } 0 \le \varepsilon < \varepsilon_0, \\ [k\varepsilon_0, +\infty), & \text{if } \varepsilon = \varepsilon_0, \\ \emptyset, & \text{if } \varepsilon > \varepsilon_0, \end{cases}$$

where ε_0 and k are prescribed positive constants. This law describes the behavior of a body which offers no resistance for compression, is linear (Hooke's law) for $0 < \varepsilon < \varepsilon_0$, and has an infinite jump called a locking effect for $\varepsilon = \varepsilon_0$.

Note that variational problems encountered in the theory of locking materials were studied in [9], where the equivalence between the statical and the kinematical methods for such materials was shown.

In this paper, we consider elastic materials with the following constitutive law:

$$\boldsymbol{\sigma}(\boldsymbol{u}) \in \mathcal{A}(\boldsymbol{\varepsilon}(\boldsymbol{u})) + \partial I_B(\boldsymbol{\varepsilon}(\boldsymbol{u})) \ \text{ in } \Omega, \tag{2}$$

where Ω is an open, bounded, connected set in $\mathbb{R}^d$ with a Lipschitz boundary $\partial\Omega$, $\mathcal{A} : \Omega \times \mathbb{S}^d \to \mathbb{S}^d$ is a nonlinear elasticity operator, $B \subset \mathbb{S}^d$ is a locking constraint set,

$$I_B(\boldsymbol{\varepsilon}) = \begin{cases} 0, & \text{if } \boldsymbol{\varepsilon} \in B, \\ +\infty, & \text{if } \boldsymbol{\varepsilon} \in \mathbb{S}^d \setminus B \end{cases}$$

is the indicator function of the set B, and $\partial I_B : \mathbb{S}^d \to 2^{\mathbb{S}^d}$ stands for the subdifferential of I_B. In the case where the operator $\boldsymbol{\varepsilon} \mapsto \mathcal{A}(\boldsymbol{x}, \boldsymbol{\varepsilon})$ is linear with the elasticity tensor components a_{ijkl}, the relation (2) reduces to (1). Moreover, in this case, the law (2) can be written as

$$\boldsymbol{\sigma}(\boldsymbol{u}) \in \partial w(\boldsymbol{\varepsilon}(\boldsymbol{u})) \quad \text{in } \Omega,$$

the potential function $w : \mathbb{S}^d \to \mathbb{R}$ being defined by

$$w(\boldsymbol{\varepsilon}) = \frac{1}{2}\, a_{ijkl}\, \varepsilon_{ij}\, \varepsilon_{kl} + I_B(\boldsymbol{\varepsilon}) \ \text{ for } \ \boldsymbol{\varepsilon} \in \mathbb{S}^d.$$

Several choices of the set B can be found in the literature for perfectly locking materials. As an example, $B = \{\boldsymbol{\varepsilon} \in \mathbb{S}^d \mid Q(\boldsymbol{\varepsilon}) \le 0\}$, where the locking function $Q : \mathbb{S}^d \to \mathbb{R}$ is convex, continuous, and $Q(\mathbf{0}) \le 0$. The strains are restricted by the inequality $Q(\boldsymbol{\varepsilon}) \le 0$. The choice

$$Q(\boldsymbol{\varepsilon}) = \frac{1}{2}\, \varepsilon^D_{ij}\varepsilon^D_{ij} - \kappa^2, \quad \kappa > 0 \tag{3}$$

was considered by Prager in [7] to model an ideal-locking effect. Here, $\boldsymbol{\varepsilon}^D = (\varepsilon^D_{ij})$ denotes the deviatoric part of the strain, $\varepsilon^D_{ij} = \varepsilon_{ij} - \frac{1}{d}\,\mathrm{tr}(\boldsymbol{\varepsilon})I$, $\mathrm{tr}(\boldsymbol{\varepsilon}) = \varepsilon_{ii}$ is the trace of the tensor $\boldsymbol{\varepsilon}(\boldsymbol{u})$, and I stands for the identity matrix. The choice

$$Q(\boldsymbol{\varepsilon}) = |\mathrm{tr}(\boldsymbol{\varepsilon})|^2 - \kappa^2, \quad \kappa > 0 \tag{4}$$

leads to materials with limited compressibility [7]. This choice of the locking function Q can be used to describe the behavior of rubber and some of other types of plastic materials [10]. In the limiting case $\kappa = 0$, the set B corresponds to incompressible elastic materials [9]. In modeling the torsion of a cylindrical bar made of a locking material, the set B is chosen to be the ball centered at zero with a radius $r > 0$ [9]. In one-dimensional models of idealized strain–stress law for rubber, the choice $Q(\varepsilon) = \varepsilon - \varepsilon_0$ [11,12] reflects the phenomenon that the stress can take at the locking criterion an arbitrarily large value without any change of the strain state.

The rest of the paper is organized as follows. In Section 2, we state the variational–hemivariational inequality formulation of the contact problem and recall the existence and uniqueness result proved in [5]. In Section 3, we introduce a numerical method for the variational–hemivariational inequality and derive an error bound. Finally, in Section 4, we provide numerical simulation results.

2. The variational–hemivariational inequality

In the statement of the variational–hemivariational inequality, we need the notion of the Clarke subgradient. Let $(X, \|\cdot\|_X)$ be a Banach space with its dual denoted by X^* and let $\langle\cdot,\cdot\rangle$ stand for the duality pairing of X^* and X.

Definition 1. Let $g : X \to \mathbb{R}$ be a locally Lipschitz function. The (Clarke) generalized directional derivative of g at the point $x \in X$ in the direction $v \in X$ is defined by

$$g^0(x; v) = \limsup_{y\to x,\ \lambda\downarrow 0} \frac{g(y + \lambda v) - g(y)}{\lambda}.$$

The generalized gradient (subdifferential) of g at x is a subset of the dual space X^* given by

$$\partial g(x) = \left\{\zeta \in X^* \mid g^0(x; v) \ge \langle\zeta, v\rangle \text{ for all } v \in X\right\}.$$

Detailed discussions of the Clarke generalized directional derivative and the generalized gradient can be found in [13–16].

We now recall the classical formulation of the contact problem studied in [5].

Problem 2. Find a displacement field $\boldsymbol{u} : \Omega \to \mathbb{R}^d$ and a stress field $\boldsymbol{\sigma} : \Omega \to \mathbb{S}^d$ such that

$$\boldsymbol{\sigma}(\boldsymbol{u}) \in \mathcal{A}(\boldsymbol{\varepsilon}(\boldsymbol{u})) + \partial I_B(\boldsymbol{\varepsilon}(\boldsymbol{u})) \quad \text{in } \Omega, \tag{5}$$

$$-\operatorname{Div}\boldsymbol{\sigma}(\boldsymbol{u}) = \boldsymbol{f}_0 \quad \text{in } \Omega, \tag{6}$$

$$\boldsymbol{u} = \boldsymbol{0} \quad \text{on } \Gamma_D, \tag{7}$$

$$\boldsymbol{\sigma}(\boldsymbol{u})\boldsymbol{\nu} = \boldsymbol{f}_N \quad \text{on } \Gamma_N, \tag{8}$$

$$\sigma_\nu(\boldsymbol{u}) \le 0, \quad u_\nu \le 0, \quad \sigma_\nu(\boldsymbol{u})u_\nu = 0 \quad \text{on } \Gamma_C, \tag{9}$$

$$-\boldsymbol{\sigma}_\tau(\boldsymbol{u}) \in \mu(\|\boldsymbol{u}_\tau\|)\,\partial j(\boldsymbol{u}_\tau) \quad \text{on } \Gamma_C. \tag{10}$$

The set Ω represents the elastic body in its reference configuration and it is assumed to be an open, bounded, and connected subset of $\mathbb{R}^d$, $d \le 3$. The boundary Γ of Ω is supposed to be Lipschitz continuous and therefore the outward unit normal on the boundary, denoted by $\boldsymbol{\nu} = (\nu_i)$, is defined a.e. Moreover, Γ is partitioned into three disjoint measurable parts Γ_D, Γ_N and Γ_C such that $meas(\Gamma_C) > 0$. The inner products and norms on $\mathbb{R}^d$ and $\mathbb{S}^d$ are defined by

$$\boldsymbol{u}\cdot\boldsymbol{v} = u_i v_i, \quad \|\boldsymbol{v}\| = (\boldsymbol{v}\cdot\boldsymbol{v})^{1/2} \quad \text{for all } \boldsymbol{u} = (u_i),\ \boldsymbol{v} = (v_i) \in \mathbb{R}^d,$$

$$\boldsymbol{\sigma}\cdot\boldsymbol{\tau} = \sigma_{ij}\tau_{ij}, \quad \|\boldsymbol{\tau}\| = (\boldsymbol{\tau}\cdot\boldsymbol{\tau})^{1/2} \quad \text{for all } \boldsymbol{\sigma} = (\sigma_{ij}),\ \boldsymbol{\tau} = (\tau_{ij}) \in \mathbb{S}^d,$$

respectively.

The constitutive law for elastic materials with locking constraints is given by Eq. (5). It is assumed that the contact process is static and so we use the equilibrium equation (6), $\boldsymbol{f}_0$ being the body force density. Conditions (7) and (8) are the classical displacement and traction boundary conditions: the body is fixed on Γ_D and surface tractions of density $\boldsymbol{f}_N$ are applied on Γ_N. The Signorini contact condition in its classical form without gap is given by relation (9) which holds on the surface Γ_C. Here, σ_ν and $\boldsymbol{\sigma}_\tau$ represent the normal and tangential components of the stress field $\boldsymbol{\sigma}$ on the boundary, and are defined by $\sigma_\nu = (\boldsymbol{\sigma}\boldsymbol{\nu})\cdot\boldsymbol{\nu}$ and $\boldsymbol{\sigma}_\tau = \boldsymbol{\sigma}\boldsymbol{\nu} - \sigma_\nu\boldsymbol{\nu}$. The normal and tangential components of a vector field $\boldsymbol{v}$ on the boundary are given by $v_\nu = \boldsymbol{v}\cdot\boldsymbol{\nu}$ and $\boldsymbol{v}_\tau = \boldsymbol{v} - v_\nu\boldsymbol{\nu}$, respectively. Relation (9) is a unilateral contact condition which assumes that the foundation is perfectly rigid. Finally, condition (10) represents the friction law, in which ∂j denotes the generalized gradient of the prescribed function j, and μ is the friction coefficient, assumed to be a positive function on Γ_C. We allow the function μ to depend on the slip, i.e. the tangential displacement. Details on mechanical description of static contact models with elastic materials can be found in the books [17,18,15].

We need the following hypotheses on the elasticity operator $\mathcal{A}$ and the locking constraint set B.

$$\left\{\begin{array}{l}\mathcal{A}:\Omega\times\mathbb{S}^d\to\mathbb{S}^d \text{ is such that}\\ \text{(a) } \mathcal{A}(\cdot,\boldsymbol{\varepsilon}) \text{ is measurable on } \Omega \text{ for all } \boldsymbol{\varepsilon}\in\mathbb{S}^d;\\ \text{(b) } \mathcal{A}(\boldsymbol{x},\cdot) \text{ is continuous on } \mathbb{S}^d \text{ for a.e. } \boldsymbol{x}\in\Omega;\\ \text{(c) there exist } a_0\in L^2(\Omega),\ a_0\ge 0 \text{ and } a_1>0 \text{ such that}\\ \qquad \|\mathcal{A}(\boldsymbol{x},\boldsymbol{\varepsilon})\|\le a_0(\boldsymbol{x})+a_1\|\boldsymbol{\varepsilon}\| \quad \text{for all } \boldsymbol{\varepsilon}\in\mathbb{S}^d,\ \text{a.e. } \boldsymbol{x}\in\Omega;\\ \text{(d) there exists } m_{\mathcal{A}}>0 \text{ such that}\\ \qquad (\mathcal{A}(\boldsymbol{x},\boldsymbol{\varepsilon}_1)-\mathcal{A}(\boldsymbol{x},\boldsymbol{\varepsilon}_2))\cdot(\boldsymbol{\varepsilon}_1-\boldsymbol{\varepsilon}_2)\ge m_{\mathcal{A}}\,\|\boldsymbol{\varepsilon}_1-\boldsymbol{\varepsilon}_2\|^2\\ \qquad\quad \text{for all } \boldsymbol{\varepsilon}_1,\boldsymbol{\varepsilon}_2\in\mathbb{S}^d,\ \text{a.e. } \boldsymbol{x}\in\Omega;\\ \text{(e) } \mathcal{A}(\boldsymbol{x},\boldsymbol{0}_{\mathbb{S}^d})=\boldsymbol{0}_{\mathbb{S}^d} \text{ for a.e. } \boldsymbol{x}\in\Omega.\end{array}\right. \tag{11}$$

$$B \text{ is a closed, convex subset of } \mathbb{S}^d \text{ with } \boldsymbol{0}_{\mathbb{S}^d}\in B. \tag{12}$$

The potential function j and the friction coefficient μ are assumed to satisfy the following conditions.

$$\left\{\begin{array}{l} j:\Gamma_C\times\mathbb{R}^d\to\mathbb{R} \text{ is such that}\\ \text{(a) } j(\cdot,\boldsymbol{\xi}) \text{ is measurable on } \Gamma_C \text{ for all } \boldsymbol{\xi}\in\mathbb{R}^d \text{ and there}\\ \qquad \text{exists } \overline{e}\in L^2(\Gamma_C;\mathbb{R}^d) \text{ such that } j(\cdot,\overline{e}(\cdot))\in L^1(\Gamma_C);\\ \text{(b) } j(\boldsymbol{x},\cdot) \text{ is locally Lipschitz on } \mathbb{R}^d \text{ for a.e. } \boldsymbol{x}\in\Gamma_C;\\ \text{(c) } \|\partial j(\boldsymbol{x},\boldsymbol{\xi})\|\le c_j \text{ for all } \boldsymbol{\xi}\in\mathbb{R}^d,\ \text{a.e. } \boldsymbol{x}\in\Gamma_C \text{ with } c_j>0;\\ \text{(d) } j^0(\boldsymbol{x},\boldsymbol{\xi}_1;\boldsymbol{\xi}_2-\boldsymbol{\xi}_1)+j^0(\boldsymbol{x},\boldsymbol{\xi}_2;\boldsymbol{\xi}_1-\boldsymbol{\xi}_2)\le\alpha_j\,\|\boldsymbol{\xi}_1-\boldsymbol{\xi}_2\|^2\\ \qquad \text{for all } \boldsymbol{\xi}_1,\ \boldsymbol{\xi}_2\in\mathbb{R}^d, \text{ a.e. } \boldsymbol{x}\in\Gamma_C \text{ with } \alpha_j\ge 0.\end{array}\right. \tag{13}$$

$$\left\{\begin{array}{l} \mu:\Gamma_C\times\mathbb{R}_+\to\mathbb{R}_+ \text{ is such that}\\ \text{(a) there exists } L_\mu>0 \text{ such that}\\ \qquad |\mu(\boldsymbol{x},r_1)-\mu(\boldsymbol{x},r_2)|\le L_\mu|r_1-r_2|\\ \qquad\quad \text{for all } r_1,r_2\in\mathbb{R}_+,\ \text{a.e. } \boldsymbol{x}\in\Gamma_C;\\ \text{(b) } \mu(\cdot,r) \text{ is measurable on } \Gamma_C \text{ for all } r\in\mathbb{R};\\ \text{(c) there exists } \mu_0>0 \text{ such that } \mu(\boldsymbol{x},r)\le\mu_0\\ \qquad \text{for all } r\in\mathbb{R}_+,\ \text{a.e. } \boldsymbol{x}\in\Gamma_C.\end{array}\right. \tag{14}$$

The condition (13)(d) is equivalent to the relaxed monotonicity condition

$$(\partial j(\boldsymbol{x},\boldsymbol{\xi}_1)-\partial j(\boldsymbol{x},\boldsymbol{\xi}_2))\cdot(\boldsymbol{\xi}_1-\boldsymbol{\xi}_2)\ge-\alpha_j\|\boldsymbol{\xi}_1-\boldsymbol{\xi}_2\|^2 \tag{15}$$

for all $\boldsymbol{\xi}_1,\boldsymbol{\xi}_2\in\mathbb{R}^d$, a.e. $\boldsymbol{x}\in\Gamma_C$. In the case where $j(\boldsymbol{x},\cdot)$ is a convex function, $\alpha_j=0$ and this condition reduces to the monotonicity of the convex subdifferential.

Furthermore, we assume that the densities of body forces and surface tractions have the following regularity

$$\boldsymbol{f}_0\in L^2(\Omega;\mathbb{R}^d),\quad \boldsymbol{f}_N\in L^2(\Gamma_N;\mathbb{R}^d). \tag{16}$$

We give two examples for the function j in the friction condition (10). For simplicity, we skip the dependence of the potential $j:\mathbb{R}^d\to\mathbb{R}$ on the $\boldsymbol{x}$ variable. More examples for the function j can be found in [15, Chapter 7].

The first example is

$$j(\boldsymbol{\xi})=\begin{cases} a\,\|\boldsymbol{\xi}\|+\dfrac{a(1-a)}{2} & \text{if } \|\boldsymbol{\xi}\|\ge a,\\ \dfrac{a-1}{2a}\|\boldsymbol{\xi}\|^2+\|\boldsymbol{\xi}\| & \text{if } \|\boldsymbol{\xi}\|\le a\end{cases} \tag{17}$$

for $\boldsymbol{\xi}\in\mathbb{R}^d$, where $0<a<1$ is given. Its subdifferential is

$$\partial j(\boldsymbol{\xi})=\begin{cases} a\,\dfrac{\boldsymbol{\xi}}{\|\boldsymbol{\xi}\|} & \text{if } \|\boldsymbol{\xi}\|\ge a,\\ \overline{B}(\boldsymbol{0},1) & \text{if } \boldsymbol{\xi}=\boldsymbol{0},\\ \dfrac{a-1}{a}\,\boldsymbol{\xi}+\dfrac{\boldsymbol{\xi}}{\|\boldsymbol{\xi}\|} & \text{if } 0<\|\boldsymbol{\xi}\|\le a\end{cases}$$

for $\boldsymbol{\xi}\in\mathbb{R}^d$, where $\overline{B}(\boldsymbol{0},1)$ is the closed unit ball in $\mathbb{R}^d$. The function j is nonconvex and it satisfies hypotheses (13) with $c_j=1$ and $\alpha_j=1$ [15]. The corresponding friction law (10) takes the form

$$\begin{cases} \|\boldsymbol{\sigma}_\tau\|\le\mu(0) & \text{if } \boldsymbol{u}_\tau=\boldsymbol{0},\\ -\boldsymbol{\sigma}_\tau=\mu(\|\boldsymbol{u}_\tau\|)\Big(\dfrac{a-1}{a}\,\boldsymbol{u}_\tau+\dfrac{\boldsymbol{u}_\tau}{\|\boldsymbol{u}_\tau\|}\Big) & \text{if } 0<\|\boldsymbol{u}_\tau\|\le a,\\ -\boldsymbol{\sigma}_\tau=\mu(\|\boldsymbol{u}_\tau\|)a\dfrac{\boldsymbol{u}_\tau}{\|\boldsymbol{u}_\tau\|} & \text{if } \|\boldsymbol{u}_\tau\|\ge a\end{cases} \tag{18}$$

on Γ_C. If $a = 1$ in (17), the function $j(\boldsymbol{\xi}) = \|\boldsymbol{\xi}\|$ is convex and the friction law (18) becomes the classical Coulomb's law of dry friction. The latter has been studied in several monographs, cf. [19,17,15,18,20].

As another example, consider

$$j(\boldsymbol{\xi}) = \sqrt{\|\boldsymbol{\xi}\|^2 + \rho^2} - \rho \quad \text{for} \quad \boldsymbol{\xi} \in \mathbb{R}^d,$$

where $\rho > 0$ is a parameter. This function is convex and continuously differentiable, and

$$\partial j(\boldsymbol{\xi}) = j'(\boldsymbol{\xi}) = \frac{\boldsymbol{\xi}}{\sqrt{\|\boldsymbol{\xi}\|^2 + \rho^2}} \quad \text{for} \quad \boldsymbol{\xi} \in \mathbb{R}^d. \tag{19}$$

The function j satisfies (13)(b), (13)(c) with $c_j = 1$ and ∂j is monotone, i.e., (13)(d) holds with $\alpha_j = 0$. The corresponding friction condition (10) reduces to the static version of the regularized Coulomb friction law with slip:

$$-\boldsymbol{\sigma}_\tau(\boldsymbol{u}) = \mu(\|\boldsymbol{u}_\tau\|)\frac{\boldsymbol{u}_\tau}{\sqrt{\|\boldsymbol{u}_\tau\|^2 + \rho^2}} \quad \text{on} \quad \Gamma_C.$$

Returning to Problem 2, for its weak formulation, we introduce some function spaces:

$$V = \{\, \boldsymbol{v} \in H^1(\Omega; \mathbb{R}^d) \mid \boldsymbol{v} = \boldsymbol{0} \text{ on } \Gamma_D \,\}, \quad H = L^2(\Omega; \mathbb{R}^d), \quad \mathcal{H} = L^2(\Omega; \mathbb{S}^d).$$

These are Hilbert spaces. The inner product over the space $\mathcal{H}$ is

$$\langle \boldsymbol{\sigma}, \boldsymbol{\tau} \rangle_{\mathcal{H}} = \int_\Omega \sigma_{ij}(\boldsymbol{x})\, \tau_{ij}(\boldsymbol{x})\, dx.$$

The inner product over the space V is

$$\langle \boldsymbol{u}, \boldsymbol{v} \rangle_V = \langle \boldsymbol{\varepsilon}(\boldsymbol{u}), \boldsymbol{\varepsilon}(\boldsymbol{v}) \rangle_{\mathcal{H}} \quad \text{for} \quad \boldsymbol{u}, \boldsymbol{v} \in V,$$

recalling that meas$\,(\Gamma_D) > 0$. For $\boldsymbol{v} \in V$, we denote its trace on the boundary by the same symbol $\boldsymbol{v}$. The trace operator is continuous,

$$\|\boldsymbol{v}\|_{L^2(\partial\Omega;\mathbb{R}^d)} \le \|\gamma\|\, \|\boldsymbol{v}\|_V \text{ for all } \boldsymbol{v} \in V,$$

where $\|\gamma\|$ denotes the norm of the trace operator $\gamma : V \to L^2(\partial\Omega; \mathbb{R}^d)$. Define $\boldsymbol{f} \in V^*$ by

$$\langle \boldsymbol{f}, \boldsymbol{v} \rangle = \langle \boldsymbol{f}_0, \boldsymbol{v} \rangle_H + \langle \boldsymbol{f}_N, \boldsymbol{v} \rangle_{L^2(\Gamma_N;\mathbb{R}^d)} \quad \text{for all } \boldsymbol{v} \in V, \tag{20}$$

the set of admissible displacement fields

$$K_1 = \{\, \boldsymbol{v} \in V \mid v_\nu \le 0 \ \text{ on } \Gamma_C \,\}, \tag{21}$$

and the set with locking constraint

$$K_2 = \{\, \boldsymbol{v} \in V \mid \boldsymbol{\varepsilon}(\boldsymbol{v}(\boldsymbol{x})) \in B \text{ a.e. } \boldsymbol{x} \in \Omega \,\}. \tag{22}$$

Note that for the choice (4),

$$K_2 = \{\boldsymbol{v} \in V \mid \operatorname{div} \boldsymbol{v}(\boldsymbol{x}) \in [-\kappa, \kappa] \text{ a.e. } \boldsymbol{x} \in \Omega\}.$$

Further define

$$K = K_1 \cap K_2 \tag{23}$$

which is a closed and convex set with $\boldsymbol{0}_V \in K$. Then, the weak formulation of Problem 2 is the following.

Problem 3. Find a displacement field $\boldsymbol{u} \in K$ such that

$$\begin{aligned} &\langle \mathcal{A}(\boldsymbol{\varepsilon}(\boldsymbol{u})), \boldsymbol{\varepsilon}(\boldsymbol{v}) - \boldsymbol{\varepsilon}(\boldsymbol{u}) \rangle_{\mathcal{H}} + \int_{\Gamma_C} \mu(\|\boldsymbol{u}_\tau\|) j^0(\boldsymbol{u}_\tau; \boldsymbol{v}_\tau - \boldsymbol{u}_\tau)\, d\Gamma \\ &\quad \ge \langle \boldsymbol{f}, \boldsymbol{v} - \boldsymbol{u} \rangle_{V^* \times V} \quad \text{for all} \ \ \boldsymbol{v} \in K. \end{aligned} \tag{24}$$

Using the indicator function I_{K_2}, we can rephrase Problem 3 as one to find $\boldsymbol{u} \in K_1$ such that

$$\begin{aligned} &\langle \mathcal{A}(\boldsymbol{\varepsilon}(\boldsymbol{u})), \boldsymbol{\varepsilon}(\boldsymbol{v}) - \boldsymbol{\varepsilon}(\boldsymbol{u}) \rangle_{\mathcal{H}} + I_{K_2}(\boldsymbol{v}) - I_{K_2}(\boldsymbol{u}) + \int_{\Gamma_C} \mu(\|\boldsymbol{u}_\tau\|) j^0(\boldsymbol{u}_\tau; \boldsymbol{v}_\tau - \boldsymbol{u}_\tau)\, d\Gamma \\ &\quad \ge \langle \boldsymbol{f}, \boldsymbol{v} - \boldsymbol{u} \rangle_{V^* \times V} \quad \text{for all} \ \ \boldsymbol{v} \in K_1. \end{aligned}$$

For this reason, we call Problem 3 a variational–hemivariational inequality.

The following existence and uniqueness result is proved in [5, Theorem 12].

Theorem 4. *Assume hypotheses (11)– (16) and the following smallness condition*

$$(\mu_0\,\alpha_j + c_j\,L_\mu)\|\gamma\|^2 < m_{\mathcal{A}}. \tag{25}$$

Then Problem 3 has a unique solution $\boldsymbol{u} \in K$.

3. Numerical analysis of the problem

We consider the numerical solution of Problem 3 by the finite element method in this section. For simplicity, we assume Ω is a polygonal/tetrahedral domain. Let $\{\mathcal{T}^h\}$ be a regular family of partitions of $\overline{\Omega}$ into triangles/tetrahedrons that are compatible with the partition of the boundary $\partial\Omega$ into Γ_D, Γ_N, and Γ_C, in the sense that if the intersection of one side/face of an element with one of the three sets has a positive surface measure, then the side/face lies entirely in that set. Then we construct linear element spaces corresponding to $\mathcal{T}^h$

$$V^h = \left\{ \boldsymbol{v}^h \in C(\overline{\Omega})^d \mid \boldsymbol{v}^h|_T \in \mathbb{P}_1(T)^d \text{ for } T \in \mathcal{T}^h,\ \boldsymbol{v}^h = \boldsymbol{0} \text{ on } \Gamma_D \right\},$$

where $\mathbb{P}_1(T)$ stands for the space of polynomials of a degree less than or equal to 1 on T. Let

$$K^h = \left\{ \boldsymbol{v}^h \in V \mid v^h_\nu \le 0 \text{ on } \Gamma_C,\ \boldsymbol{\varepsilon}(\boldsymbol{v}^h) \in B \text{ in } \Omega \right\}. \tag{26}$$

The set K^h is non-empty since $\boldsymbol{0} \in K^h$. Then the finite element method for Problem 3 is the following.

Problem 5. Find $\boldsymbol{u}^h \in K^h$ such that

$$\begin{aligned}\langle \mathcal{A}(\boldsymbol{\varepsilon}(\boldsymbol{u}^h)), \boldsymbol{\varepsilon}(\boldsymbol{v}^h) - \boldsymbol{\varepsilon}(\boldsymbol{u}^h)\rangle_{\mathcal{H}} &+ \int_{\Gamma_C} \mu(\|\boldsymbol{u}^h_\tau\|) j^0(\boldsymbol{u}^h_\tau; \boldsymbol{v}^h_\tau - \boldsymbol{u}^h_\tau)\, d\Gamma \\ &\ge \langle \boldsymbol{f}, \boldsymbol{v}^h - \boldsymbol{u}^h\rangle_{V^*\times V} \quad \text{for all } \boldsymbol{v}^h \in K^h.\end{aligned} \tag{27}$$

The proof of Theorem 4 from [5] can be carried over to show that Problem 5 has a unique solution $\boldsymbol{u}^h \in K^h$. The focus of this section is to derive error estimates.

For error analysis, in addition to the previously stated assumptions on the data, we also assume that $\mathcal{A} : \Omega \times \mathbb{S}^d \to \mathbb{S}^d$ is Lipschitz continuous:

$$\|\mathcal{A}\boldsymbol{\varepsilon}_1 - \mathcal{A}\boldsymbol{\varepsilon}_2\| \le L_{\mathcal{A}}\, \|\boldsymbol{\varepsilon}_1 - \boldsymbol{\varepsilon}_2\| \ \text{ for all } \ \boldsymbol{\varepsilon}_1, \boldsymbol{\varepsilon}_2 \in \mathbb{S}^d \ \text{ with } \ L_{\mathcal{A}} > 0. \tag{28}$$

We start with an application of (11)(d) which gives

$$m_{\mathcal{A}}\|\boldsymbol{u} - \boldsymbol{u}^h\|_V^2 \le \langle \mathcal{A}(\boldsymbol{\varepsilon}(\boldsymbol{u})) - \mathcal{A}(\boldsymbol{\varepsilon}(\boldsymbol{u}^h)), \boldsymbol{\varepsilon}(\boldsymbol{u} - \boldsymbol{u}^h)\rangle_{\mathcal{H}}.$$

For any $\boldsymbol{v}^h \in K^h$, we rewrite the above inequality as

$$\begin{aligned} m_{\mathcal{A}}\|\boldsymbol{u} - \boldsymbol{u}^h\|_V^2 \le\ & \langle \mathcal{A}(\boldsymbol{\varepsilon}(\boldsymbol{u})) - \mathcal{A}(\boldsymbol{\varepsilon}(\boldsymbol{u}^h)), \boldsymbol{\varepsilon}(\boldsymbol{u} - \boldsymbol{v}^h)\rangle_{\mathcal{H}} + \langle \mathcal{A}(\boldsymbol{\varepsilon}(\boldsymbol{u})), \boldsymbol{\varepsilon}(\boldsymbol{v}^h - \boldsymbol{u})\rangle_{\mathcal{H}} \\ & + \langle \mathcal{A}(\boldsymbol{\varepsilon}(\boldsymbol{u})), \boldsymbol{\varepsilon}(\boldsymbol{u} - \boldsymbol{u}^h)\rangle_{\mathcal{H}} + \langle \mathcal{A}(\boldsymbol{\varepsilon}(\boldsymbol{u}^h)), \boldsymbol{\varepsilon}(\boldsymbol{u}^h - \boldsymbol{v}^h)\rangle_{\mathcal{H}}. \end{aligned} \tag{29}$$

From (24) with $\boldsymbol{v} = \boldsymbol{u}^h$, we have

$$\langle \mathcal{A}(\boldsymbol{\varepsilon}(\boldsymbol{u})), \boldsymbol{\varepsilon}(\boldsymbol{u} - \boldsymbol{u}^h)\rangle_{\mathcal{H}} \le \int_{\Gamma_C} \mu(\|\boldsymbol{u}_\tau\|) j^0(\boldsymbol{u}_\tau; \boldsymbol{u}^h_\tau - \boldsymbol{u}_\tau)\, d\Gamma - \langle \boldsymbol{f}, \boldsymbol{u}^h - \boldsymbol{u}\rangle_{V^*\times V}.$$

From (27), we obtain

$$\langle \mathcal{A}(\boldsymbol{\varepsilon}(\boldsymbol{u}^h)), \boldsymbol{\varepsilon}(\boldsymbol{u}^h - \boldsymbol{v}^h)\rangle_{\mathcal{H}} \le \int_{\Gamma_C} \mu(\|\boldsymbol{u}^h_\tau\|) j^0(\boldsymbol{u}^h_\tau; \boldsymbol{v}^h_\tau - \boldsymbol{u}^h_\tau)\, d\Gamma - \langle \boldsymbol{f}, \boldsymbol{v}^h - \boldsymbol{u}^h\rangle_{V^*\times V}.$$

Use these two inequalities in (29), after some rearrangement of the terms, to get

$$m_{\mathcal{A}}\|\boldsymbol{u} - \boldsymbol{u}^h\|_V^2 \le \langle \mathcal{A}(\boldsymbol{\varepsilon}(\boldsymbol{u})) - \mathcal{A}(\boldsymbol{\varepsilon}(\boldsymbol{u}^h)), \boldsymbol{\varepsilon}(\boldsymbol{u} - \boldsymbol{v}^h)\rangle_{\mathcal{H}} + R(\boldsymbol{u} - \boldsymbol{v}^h) + I_j(\boldsymbol{u}_\tau, \boldsymbol{u}^h_\tau, \boldsymbol{v}^h_\tau), \tag{30}$$

where

$$R(\boldsymbol{w}) = \langle \boldsymbol{f}, \boldsymbol{w}\rangle_{V^*\times V} - \langle \mathcal{A}(\boldsymbol{\varepsilon}(\boldsymbol{u})), \boldsymbol{\varepsilon}(\boldsymbol{w})\rangle_{\mathcal{H}} + \int_{\Gamma_C} \mu(\|\boldsymbol{u}_\tau\|) j^0(\boldsymbol{u}_\tau; -\boldsymbol{w}_\tau)\, d\Gamma, \tag{31}$$

$$\begin{aligned} I_j(\boldsymbol{u}_\tau, \boldsymbol{u}^h_\tau, \boldsymbol{v}^h_\tau) = \int_{\Gamma_C} \Big[& \mu(\|\boldsymbol{u}_\tau\|) \left(j^0(\boldsymbol{u}_\tau; \boldsymbol{u}^h_\tau - \boldsymbol{u}_\tau) - j^0(\boldsymbol{u}_\tau; \boldsymbol{v}^h_\tau - \boldsymbol{u}_\tau) \right) \\ & + \mu(\|\boldsymbol{u}^h_\tau\|) j^0(\boldsymbol{u}^h_\tau; \boldsymbol{v}^h_\tau - \boldsymbol{u}^h_\tau) \Big]\, d\Gamma. \end{aligned} \tag{32}$$

Next, we write

$$\mu(\|\boldsymbol{u}_\tau^h\|)j^0(\boldsymbol{u}_\tau^h;\boldsymbol{v}_\tau^h-\boldsymbol{u}_\tau^h)=\mu(\|\boldsymbol{u}_\tau\|)j^0(\boldsymbol{u}_\tau^h;\boldsymbol{v}_\tau^h-\boldsymbol{u}_\tau^h)\\ +\big(\mu(\|\boldsymbol{u}_\tau^h\|)-\mu(\|\boldsymbol{u}_\tau\|)\big)j^0(\boldsymbol{u}_\tau^h;\boldsymbol{v}_\tau^h-\boldsymbol{u}_\tau^h).$$

By the sub-additivity of j^0 with respect to its second argument, we have

$$j^0(\boldsymbol{u}_\tau^h;\boldsymbol{v}_\tau^h-\boldsymbol{u}_\tau^h)\le j^0(\boldsymbol{u}_\tau^h;\boldsymbol{v}_\tau^h-\boldsymbol{u}_\tau)+j^0(\boldsymbol{u}_\tau^h;\boldsymbol{u}_\tau-\boldsymbol{u}_\tau^h).$$

Then,

$$\mu(\|\boldsymbol{u}_\tau^h\|)j^0(\boldsymbol{u}_\tau^h;\boldsymbol{v}_\tau^h-\boldsymbol{u}_\tau^h)\le\mu(\|\boldsymbol{u}_\tau\|)\big(j^0(\boldsymbol{u}_\tau^h;\boldsymbol{v}_\tau^h-\boldsymbol{u}_\tau)+j^0(\boldsymbol{u}_\tau^h;\boldsymbol{u}_\tau-\boldsymbol{u}_\tau^h)\big)\\ +\big(\mu(\|\boldsymbol{u}_\tau^h\|)-\mu(\|\boldsymbol{u}_\tau\|)\big)j^0(\boldsymbol{u}_\tau^h;\boldsymbol{v}_\tau^h-\boldsymbol{u}_\tau^h),$$

and

$$I_j(\boldsymbol{u}_\tau,\boldsymbol{u}_\tau^h,\boldsymbol{v}_\tau^h)\le\int_{\Gamma_C}\Big[\mu(\|\boldsymbol{u}_\tau\|)\big(j^0(\boldsymbol{u}_\tau;\boldsymbol{u}_\tau^h-\boldsymbol{u}_\tau)+j^0(\boldsymbol{u}_\tau^h;\boldsymbol{u}_\tau-\boldsymbol{u}_\tau^h)\big)\\ +\mu(\|\boldsymbol{u}_\tau\|)\big(j^0(\boldsymbol{u}_\tau^h;\boldsymbol{v}_\tau^h-\boldsymbol{u}_\tau)-j^0(\boldsymbol{u}_\tau;\boldsymbol{v}_\tau^h-\boldsymbol{u}_\tau)\big)\\ +\big(\mu(\|\boldsymbol{u}_\tau^h\|)-\mu(\|\boldsymbol{u}_\tau\|)\big)j^0(\boldsymbol{u}_\tau^h;\boldsymbol{v}_\tau^h-\boldsymbol{u}_\tau^h)\Big]\,d\Gamma.$$

By (13)(d), it is clear that

$$j^0(\boldsymbol{u}_\tau;\boldsymbol{u}_\tau^h-\boldsymbol{u}_\tau)+j^0(\boldsymbol{u}_\tau^h;\boldsymbol{u}_\tau-\boldsymbol{u}_\tau^h)\le\alpha_j\|\boldsymbol{u}_\tau-\boldsymbol{u}_\tau^h\|^2,$$

and, by (13)(c), we deduce the following inequalities

$$\big|j^0(\boldsymbol{u}_\tau^h;\boldsymbol{v}_\tau^h-\boldsymbol{u}_\tau)\big|\le c_j\|\boldsymbol{u}_\tau-\boldsymbol{v}_\tau^h\|,\\ \big|j^0(\boldsymbol{u}_\tau;\boldsymbol{v}_\tau^h-\boldsymbol{u}_\tau)\big|\le c_j\|\boldsymbol{u}_\tau-\boldsymbol{v}_\tau^h\|,\\ \big|j^0(\boldsymbol{u}_\tau^h;\boldsymbol{v}_\tau^h-\boldsymbol{u}_\tau^h)\big|\le c_j\|\boldsymbol{v}_\tau^h-\boldsymbol{u}_\tau^h\|.$$

Subsequently, from (14)(a), it follows

$$\big|\mu(\|\boldsymbol{u}_\tau^h\|)-\mu(\|\boldsymbol{u}_\tau\|)\big|\le L_\mu\,\big|\|\boldsymbol{u}_\tau^h\|-\|\boldsymbol{u}_\tau\|\big|\le L_\mu\|\boldsymbol{u}_\tau-\boldsymbol{u}_\tau^h\|.$$

Hence, we have

$$I_j(\boldsymbol{u}_\tau,\boldsymbol{u}_\tau^h,\boldsymbol{v}_\tau^h)\le\int_{\Gamma_C}\Big[\mu_0\alpha_j\|\boldsymbol{u}_\tau-\boldsymbol{u}_\tau^h\|^2+2\mu_0c_j\|\boldsymbol{u}_\tau-\boldsymbol{v}_\tau^h\|\\ +L_\mu c_j\|\boldsymbol{u}_\tau-\boldsymbol{u}_\tau^h\|\,\|\boldsymbol{u}_\tau^h-\boldsymbol{v}_\tau^h\|\Big]\,d\Gamma.$$

Now, we use the inequality

$$\|\boldsymbol{u}_\tau^h-\boldsymbol{v}_\tau^h\|\le\|\boldsymbol{u}_\tau-\boldsymbol{u}_\tau^h\|+\|\boldsymbol{u}_\tau-\boldsymbol{v}_\tau^h\|.$$

Let $\epsilon>0$ be a small parameter. Then,

$$L_\mu c_j\|\boldsymbol{u}_\tau-\boldsymbol{u}_\tau^h\|\,\|\boldsymbol{u}_\tau^h-\boldsymbol{v}_\tau^h\|\le L_\mu c_j\|\boldsymbol{u}_\tau-\boldsymbol{u}_\tau^h\|\big(\|\boldsymbol{u}_\tau-\boldsymbol{u}_\tau^h\|+\|\boldsymbol{u}_\tau-\boldsymbol{v}_\tau^h\|\big)\\ \le\big(L_\mu c_j+\epsilon\big)\|\boldsymbol{u}_\tau-\boldsymbol{u}_\tau^h\|^2+c\,\|\boldsymbol{u}_\tau-\boldsymbol{v}_\tau^h\|^2$$

for a constant c depending on ϵ. For another constant c depending on ϵ, we have

$$\langle\mathcal{A}(\boldsymbol{\varepsilon}(\boldsymbol{u}))-\mathcal{A}(\boldsymbol{\varepsilon}(\boldsymbol{u}^h)),\boldsymbol{\varepsilon}(\boldsymbol{u}-\boldsymbol{v}^h)\rangle\le\epsilon\,\|\boldsymbol{u}-\boldsymbol{u}^h\|_V^2+c\,\|\boldsymbol{u}-\boldsymbol{v}^h\|_V^2.$$

Using these bounds in (30), we obtain

$$\big(m_{\mathcal{A}}-\big(\mu_0\alpha_j+c_jL_\mu+\epsilon\big)\|\gamma\|^2-\epsilon\big)\|\boldsymbol{u}-\boldsymbol{u}^h\|_V^2\\ \le c\,\|\boldsymbol{u}-\boldsymbol{v}^h\|_V^2+R(\boldsymbol{u}-\boldsymbol{v}^h)+c\,\|\boldsymbol{u}_\tau-\boldsymbol{v}_\tau^h\|_{L^2(\Gamma_C)}.$$

Recall the smallness condition

$$\big(\mu_0\alpha_j+c_jL_\mu\big)\|\gamma\|^2<m_{\mathcal{A}}.$$

Then for $\epsilon>0$ sufficiently small, we conclude

$$\|\boldsymbol{u}-\boldsymbol{u}^h\|_V\le c\left[\|\boldsymbol{u}-\boldsymbol{v}^h\|_V+|R(\boldsymbol{u}-\boldsymbol{v}^h)|^{1/2}+\|\boldsymbol{u}_\tau-\boldsymbol{v}_\tau^h\|_{L^2(\Gamma_C)}^{1/2}\right].\tag{33}$$

This Céa type inequality is the starting point for convergence and error estimation.

Recalling the definition (31) for $R(\boldsymbol{w})$, we can easily find a crude upper bound,

$$|R(\boldsymbol{w})| \le c \left(\|\boldsymbol{f}\|_{V^*} + \|a_0\|_{L^2(\Omega)} + \|\boldsymbol{u}\|_V + \mu_0 c_j\right) \|\boldsymbol{w}\|_V \quad \text{for all } \boldsymbol{w} \in V.$$

Consequently, from (33), we immediately have the following error bound

$$\|\boldsymbol{u} - \boldsymbol{u}^h\|_V \le c \inf_{\boldsymbol{v}^h \in K^h} \|\boldsymbol{u} - \boldsymbol{v}^h\|_V^{1/2}. \tag{34}$$

To proceed further, we make an assumption on the constraint set B: there exists a constant $c_1 > 0$ such that

$$\delta B + (1 - \delta)\, c_1 B_0 \subset B \quad \text{for all } \delta \in (0, 1). \tag{35}$$

Here, B_0 is the unit ball centered at the origin in $\mathbb{S}^d$. This assumption is valid in applications, and in particular, for the choices (3) and (4).

For the regularity of the solution $\boldsymbol{u}$, we assume that

$$\boldsymbol{u} \in W^{2,\infty}(\Omega; \mathbb{R}^d). \tag{36}$$

By the Sobolev embedding theorem, $\boldsymbol{u} \in C(\overline{\Omega}; \mathbb{R}^d)$ and so its finite element interpolant $I^h\boldsymbol{u} \in V^h$ is well defined. By the standard finite element approximation theory (see [21, Theorem 4.4.20]), there is a constant $c_2 > 0$ such that

$$\max_{T \in \mathcal{T}^h} \|\boldsymbol{u} - I^h\boldsymbol{u}\|_{W^{1,\infty}(T;\mathbb{R}^d)} \le c_2 h\, \|\boldsymbol{u}\|_{W^{2,\infty}(\Omega;\mathbb{R}^d)},$$

which implies

$$\max_{T \in \mathcal{T}^h} \|\boldsymbol{\varepsilon}(I^h\boldsymbol{u} - \boldsymbol{u})\|_{L^\infty(T;\mathbb{S}^d)} \le c_3 h\, \|\boldsymbol{u}\|_{W^{2,\infty}(\Omega;\mathbb{R}^d)} \tag{37}$$

for a suitable constant c_3 depending on c_2.

Note that $I^h\boldsymbol{u} \in K_1$. Fix $\alpha < 1$ an arbitrary positive number, and define

$$\boldsymbol{w}^h = (1 - h^\alpha)\, I^h\boldsymbol{u}. \tag{38}$$

Writing

$$\boldsymbol{\varepsilon}(\boldsymbol{w}^h) = (1 - h^\alpha)\, \boldsymbol{\varepsilon}(\boldsymbol{u}) + (1 - h^\alpha)\, \boldsymbol{\varepsilon}(I^h\boldsymbol{u} - \boldsymbol{u}),$$

by (35) with $\delta = 1 - h^\alpha$ and (37), we know that for h small enough, $\boldsymbol{w}^h \in K_2$, and then also

$$\boldsymbol{w}^h \in K^h.$$

Therefore, from (34), we have

$$\|\boldsymbol{u} - \boldsymbol{u}^h\|_V \le c\, \|\boldsymbol{u} - \boldsymbol{w}^h\|_V^{1/2}.$$

Now, exploiting the inequality

$$\begin{aligned}
\|\boldsymbol{u} - \boldsymbol{w}^h\|_V &\le \|\boldsymbol{u} - I^h\boldsymbol{u}\|_V + h^\alpha \|I^h\boldsymbol{u}\|_V \\
&\le \|\boldsymbol{u} - I^h\boldsymbol{u}\|_V + h^\alpha \left(\|\boldsymbol{u}\|_V + \|\boldsymbol{u} - I^h\boldsymbol{u}\|_V\right) \\
&\le c\, h + h^\alpha \left(\|\boldsymbol{u}\|_V + c\, h\right),
\end{aligned}$$

we have the error bound

$$\|\boldsymbol{u} - \boldsymbol{u}^h\|_V \le c\, h^{\alpha/2}, \tag{39}$$

for any $\alpha < 1$. However, we comment that the error bound (39) is not optimal in order. It is desirable to improve the error bound (39) to the optimal one

$$\|\boldsymbol{u} - \boldsymbol{u}^h\|_V \le c\, h$$

under appropriate solution regularity assumptions. This is a topic for further investigation.

4. Numerical results

In this section, we report numerical simulation results on the contact Problem 5 regularized with normal compliance and nearly locking effect, which is referred to as the regularized Problem 5 in this section.

The variational–hemivariational inequalities are usually related to the solution of nonlinear and nonconvex problems. The nonlinearities come from both the frictional contact conditions and the locking effect of the elastic material, while the nonconvexity comes from the nonmonotone dependence of the friction coefficient with respect to the tangential displacement. A classical and efficient numerical technique to solve this kind of problems is based on a “convexification”

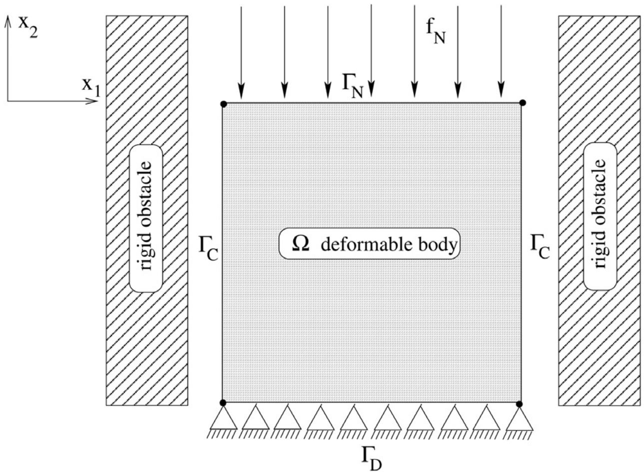

Fig. 1. Reference configuration of the two-dimensional example.

iterative procedure which leads to a sequence of convex programming problems. The solution of regularized Problem 5 based on this iterative procedure exploits numerical methods described in [22,23]. For the solution of the resulting convex iterative problems, we used classical numerical methods that can be found for instance in [24,25].

For the numerical example, we consider compression of a quasi-incompressible deformable square clamped on its horizontal bottom side and which can come into contact with two foundations on its vertical sides. The physical setting used for regularized Problem 5 is depicted in Fig. 1. The deformable body is represented by a square domain, $\Omega = (0, 4)\times(0, 4) \subset \mathbb{R}^2$, and its boundary Γ is split as follows:

$$\begin{aligned}
&\Gamma_D = [0, 4] \times \{0\},\\
&\Gamma_N = [0, 4] \times \{4\},\\
&\Gamma_C = (\{0\} \times (0, 4)) \cup (\{4\} \times (0, 4)).
\end{aligned}$$

Here, the domain Ω represents the cross section of a three-dimensional elastic body with locking effect subjected to the action of tractions in such a way that a plane stress hypothesis is assumed. On the part Γ_D the body is clamped and, therefore, the displacement field vanishes there. Vertical compression acts on the boundary Γ_N. No body force acts on the elastic body. The body is in frictional contact with two obstacles on the part Γ_C of the boundary.

The elastic locking material's behavior chosen for the numerical simulations is governed by the constitutive law of the following form

$$\boldsymbol{\sigma}(\boldsymbol{u}) = \mathcal{A}(\boldsymbol{\varepsilon}(\boldsymbol{u})) + C_\kappa(|\mathrm{tr}(\boldsymbol{\varepsilon}(\boldsymbol{u}))| - \kappa^2)_+\boldsymbol{I}, \tag{40}$$

where C_κ is a positive parameter and κ is a material constant. Note that the constitutive law (40) is based on nearly-locking effect which approximates the ideal-locking effect considered in (5). This constitutive law is related to the locking function Q introduced in Section 1 and defined by $Q(\boldsymbol{\varepsilon}) = |\mathrm{tr}(\boldsymbol{\varepsilon})| - \kappa^2$. In the model (40), C_κ represents a compliance parameter intended to tend towards infinity in order to approximate the ideal-locking effect. This nearly-locking effect can be interpreted as a quasi-limited compressibility condition that the infinitesimal strain tensor $\boldsymbol{\varepsilon}$ must satisfy (see the last remark of Section 1).

We assume that the material is homogeneous and isotropic, and the elasticity tensor $\mathcal{A}$ has the form

$$(\mathcal{A}\boldsymbol{\tau})_{ij} = \frac{E\gamma}{(1+\kappa)(1-2\gamma)}(\tau_{kk})\delta_{ij} + \frac{E}{1+\gamma}\tau_{ij}, \quad 1 \le i, j \le 2, \text{ for all } \boldsymbol{\tau} \in \mathbb{S}^2,$$

where the coefficients E and γ are Young's modulus and the Poisson's ratio of the material, respectively, and δ_{ij} denotes the Kronecker symbol. For the numerical simulation of the regularized Problem 5, the following data are used

$$\begin{aligned}
&E = 2000\, N/m^2, \quad \gamma = 0.3,\\
&C_\kappa = 10000, \quad \kappa = 0.4,\\
&\boldsymbol{f}_0 = (0, 0)\, N/m^2,\\
&\boldsymbol{f}_N = (0, -9 \times 10^2)\, N/m \text{ on } \Gamma_N.
\end{aligned}$$

The numerical results are presented in Figs. 2–4. In Fig. 2, the deformed configuration as well as the interface forces on Γ_C is plotted. In this case, the contact boundary conditions on Γ_C are characterized by a frictional contact in which the normal response follows a normal compliance law and for which the friction law is nonmonotone with respect to the

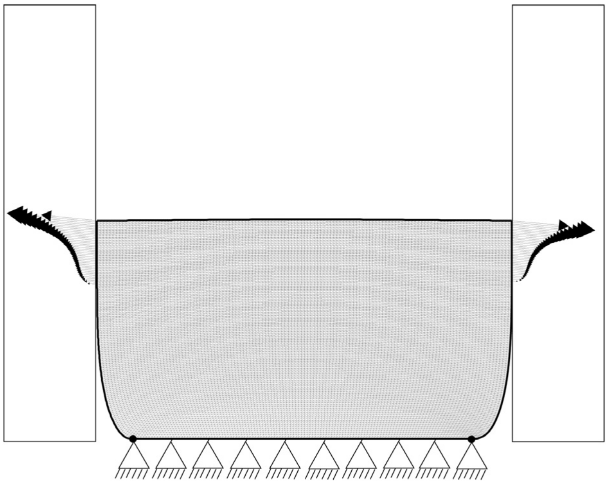

Fig. 2. Deformed mesh and interface forces on Γ_C.

tangential displacement $\boldsymbol{u}_\tau$. This nonmonotone dependence is characterized by a coefficient of friction μ which depends on the tangential displacement $\boldsymbol{u}_\tau$ as follows

$$\mu(\|\boldsymbol{u}_\tau\|) = (a - b)\, e^{-\beta\, \|\boldsymbol{u}_\tau\|} + b \tag{41}$$

with $a = 0.4$, $b = 0.1$ and $\beta = 100$, and therefore the friction bound decreases with the slip from the value a to the limit value b. As a consequence, the corresponding friction law is nonmonotone. This physical model of slip-dependent friction was introduced in [26] for earthquakes modeling in geophysics and it also was studied and used in [22,27,23,28,29]. Concerning the normal compliance contact conditions on Γ_C, we choose the following law

$$-\sigma_\nu = \begin{cases} 0 & \text{if } u_\nu < g_a, \\ c_\nu(u_\nu - g_a) & \text{if } u_\nu \geq g_a, \end{cases} \tag{42}$$

with $c_\nu = 10\,000$ and $g_a = 0.4$.

In Fig. 2, we observe that a large proportion of contact nodes situated at the top vertical extremities of Γ_C are in status of slip since the gap with the foundation and the friction bound are reached there.

In order to appreciate the locking effect, the deformed meshes as well as the interface forces on Γ_C are plotted in Fig. 3 for two values of the compliance parameter C_κ. Note that the case $C_\kappa = 0$ corresponds to the problem without locking effect. According to Fig. 3, we can see that when the compliance parameter $C_\kappa = 0$, the solution of the problem is characterized by a strong compressibility behavior that leads to no contact on the vertical sides of the square. Conversely, it is obvious to observe that the locking effect related to the quasi-limited compressibility condition considered in (40) leads to a quasi-incompressibility behavior when the compliance parameter C_κ is large ($C_\kappa = 10\,000$). Consequently, this behavior leads to the contact of several nodes located on the vertical sides of the square.

Details concerning the computation for the numerical simulations related to the solution of the regularized Problem 5 with $C_\kappa = 10\,000$ and $C_\kappa = 0$ are as follows. For instance, in Fig. 2, the problem was discretized in 33 024 finite elements with 256 contact elements; the total number of degrees of freedom was equal to 33 794. The average iterations number of the "convexification" procedure for the solution of Problem 5 was equal to 3 and the simulation runs in 76 (expressed in seconds) CPU time on an IBM computer equipped with Intel Dual core processors (Model 5148, 2.33 GHz). For comparison, the simulation for the solution of the problem without locking effect ($C_\kappa = 0$) runs in 15 CPU time.

For numerical convergence order, we computed a sequence of numerical solutions by using uniform discretization of the regularized Problem 5 with respect to the spatial discretization parameter h. For this procedure, the spatial discretization parameter h represents the surface of one finite element which is equal to the surface of the domain divided by the number of finite elastic elements. We start with $h = 1/2$ which are successively divided by 4. For instance, in Fig. 2, the numerical solution of the regularized Problem 5 is related to $h = 1/2048$.

The numerical errors in energy norm $\|\boldsymbol{u} - \boldsymbol{u}^h\|_E$ are computed for several values of the discretization parameter h. The energy norm is defined by the formula

$$\|\boldsymbol{v}^h\|_E = \frac{1}{\sqrt{2}} (\mathcal{A}(\boldsymbol{\varepsilon}(\boldsymbol{v}^h)), \boldsymbol{\varepsilon}(\boldsymbol{v}^h))^{1/2}_{\mathcal{H}}.$$

Since it is not possible to calculate the exact solution $\boldsymbol{u}$ analytically, we consider a "reference" solution $\boldsymbol{u}_{\rm ref}$ corresponding to a fine approximation of the regularized Problem 5. The numerical solution $\boldsymbol{u}_{\rm ref}$ corresponding to $h = 1/32\,768$ was taken

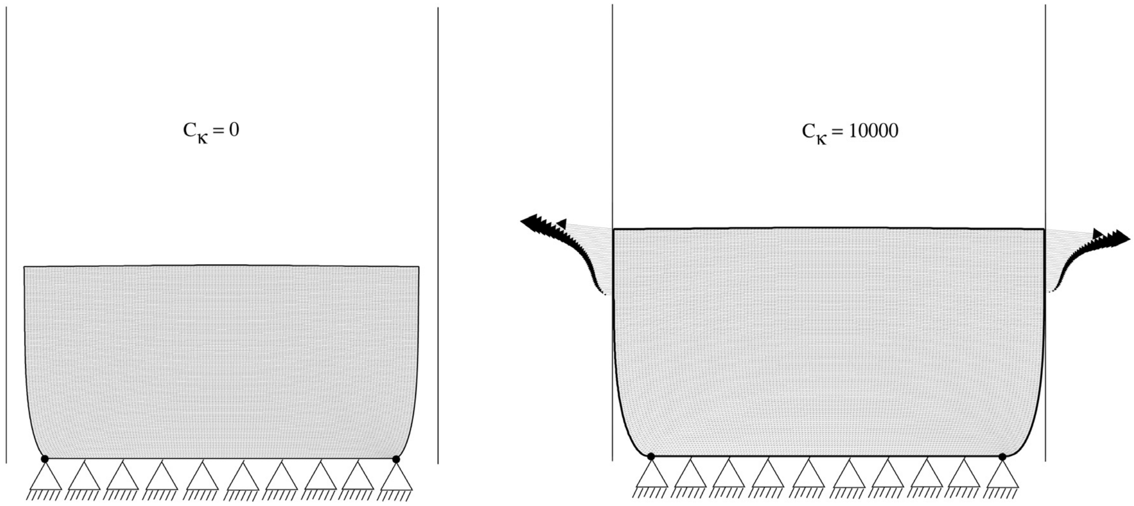

Fig. 3. Deformed meshes and interface forces on Γ_C for $C_\kappa = 0$ and $C_\kappa = 10\,000$.

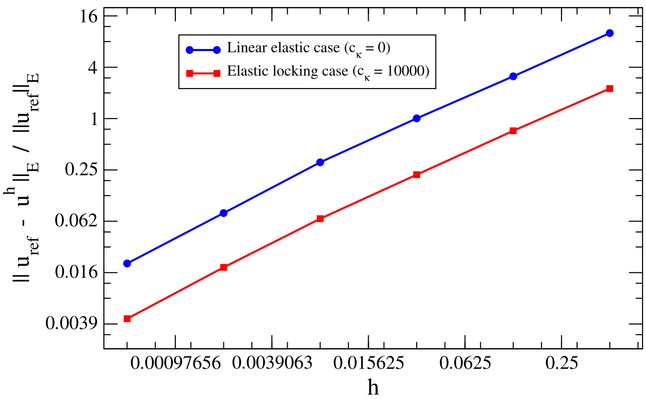

Fig. 4. Numerical errors corresponding to the regularized Problem 5 with $C_\kappa = 0$ and $C_\kappa = 10\,000$.

Table 1
Relative errors in energy norm corresponding to the regularized Problem 5 with $C_\kappa = 0$ and $C_\kappa = 10\,000$.

h	1/2	1/8	1/32	1/128	1/512	1/2048
Error for $C_\kappa = 0$	12.416%	3.974%	1.247%	0.372%	0.113%	0.021%
Error for $C_\kappa = 10\,000$	35.381%	11.028%	3.538%	1.081%	0.276%	0.070%

as the "reference" solution. This fine discretization corresponds to a problem with 528 386 degrees of freedom and 525 312 finite elements; the simulation runs in 17 894 (expressed in seconds) CPU time. The numerical results are presented in Fig. 4 and in Table 1, where the dependence of the relative error estimates $\|\boldsymbol{u}_{\mathrm{ref}} - \boldsymbol{u}^h\|_E / \|\boldsymbol{u}_{\mathrm{ref}}\|_E$ with respect to h is plotted both for the numerical solutions corresponding to the regularized Problem 5 with $C_\kappa = 0$ and $C_\kappa = 10\,000$. These results provide numerical convergence order close to 1 for the numerical solutions. We can observe that the asymptotic convergence behavior is of a similar shape for the problem with ($C_\kappa = 10\,000$) and without ($C_\kappa = 0$) the locking effect.

Acknowledgment

Research supported by the H2020-MSCA-RISE-2018 Research and Innovation Staff Exchange Scheme Fellowship, USA within the Project No. 823731 CONMECH. The work of the second author was supported by NSF (National Science Foundation), USA under grant DMS-1521684.

References

[1] W. Han, S. Migórski, M. Sofonea, A class of variational–hemivariational inequalities with applications to frictional contact problems, SIAM J. Math. Anal. 46 (2014) 3891–3912.
[2] S. Migórski, A. Ochal, M. Sofonea, History-dependent variational-hemivariational inequalities in contact mechanics, Nonlinear Anal. RWA 22 (2015) 604–618.
[3] S. Migórski, A. Ochal, M. Sofonea, A class of variational–hemivariational inequalities in reflexive Banach spaces, J. Elasticity 127 (2017) 151–178.
[4] W. Han, M. Sofonea, D. Danan, Numerical analysis of stationary variational–hemivariational inequalities, Numer. Math. 139 (2018) 563–592.
[5] S. Migórski, J. Ogorzały, A variational–hemivariational inequality in contact problem for locking materials and nonmonotone slip dependent friction, Acta Math. Sci. 37 (2017) 1639–1652.
[6] W. Prager, On ideal–locking materials, Trans. Soc. Rheol. 1 (1957) 169–175.
[7] W. Prager, Elastic solids of limited compressibility, in: Proceedings of the 9th International Congress of Applied Mechanics, Vol. 5, Brussels, 1958, pp. 205–211.
[8] W. Prager, On elastic, perfectly locking materials, in: H. Görtler (Ed.), Applied Mechanics, Proceedings of the 11th International Congress of Applied Mechanics, Munich, 1964, Springer-Verlag, Berlin, Heidelberg, 1966, pp. 538–544.
[9] F. Demengel, P. Suquet, On locking materials, Acta Appl. Math. 6 (1986) 185–211.
[10] D.W. Haines, W.D. Wilson, Strain–energy density function for rubber–like materials, J. Mech. Phys. Solids 27 (1979) 345–360.
[11] P.D. Panagiotopoulos, Inequality Problems in Mechanics and Applications, Birkhäuser, Boston, 1985.
[12] P.D. Panagiotopoulos, Hemivariational Inequalities, Applications in Mechanics and Engineering, Springer-Verlag, Berlin, 1993.
[13] F.H. Clarke, Optimization and Nonsmooth Analysis, Wiley, Interscience, New York, 1983.
[14] Z. Denkowski, S. Migórski, N.S. Papageorgiou, An Introduction to Nonlinear Analysis: Theory, Kluwer Academic/Plenum Publishers, Boston, Dordrecht, London, New York, 2003.
[15] S. Migórski, A. Ochal, M. Sofonea, Nonlinear Inclusions and Hemivariational Inequalities. Models and Analysis of Contact Problems, in: Advances in Mechanics and Mathematics, vol. 26, Springer, New York, 2013.
[16] Z. Naniewicz, P.D. Panagiotopoulos, Mathematical Theory of Hemivariational Inequalities and Applications, Marcel Dekker, Inc., New York, Basel, Hong Kong, 1995.
[17] W. Han, M. Sofonea, Quasistatic Contact Problems in Viscoelasticity and Viscoplasticity, in: Studies in Advanced Mathematics, vol. 30, Americal Mathematical Society, RI–International Press, Providence, Somerville, MA, 2002.
[18] M. Shillor, M. Sofonea, J.J. Telega, Models and Analysis of Quasistatic Contact, in: Lect. Notes Phys., vol. 655, Springer, Berlin, Heidelberg, 2004.
[19] C. Eck, J. Jarušek, M. Krbeč, Unilateral Contact Problems: Variational Methods and Existence Theorems, in: Pure and Applied Mathematics, vol. 270, Chapman/CRC Press, New York, 2005.
[20] M. Sofonea, A. Matei, Mathematical Models in Contact Mechanics, in: London Mathematical Society Lecture Note Series, vol. 398, Cambridge University Press, 2012.
[21] S.C. Brenner, L.R. Scott, The Mathematical Theory of Finite Element Methods, third ed, Springer-Verlag, New York, 2008.
[22] M. Barboteu, K. Bartosz, P. Kalita, An analytical and numerical approach to a bilateral contact problem with nonmonotone friction, Int. J. Appl. Math. Comput. Sci. 23 (2013) 263–276.
[23] M. Barboteu, K. Bartosz, P. Kalita, A. Ramadan, Analysis of a contact problem with normal compliance, finite penetration and nonmonotone slip dependent friction, Commun. Contemp. Math. 16 (2014) 1350016.
[24] T. Laursen, Computational Contact and Impact Mechanics, Springer, Berlin, 2002.
[25] P. Wriggers, Computational Contact Mechanics, second ed, Springer, Berlin, 2006.
[26] E. Rabinowicz, The nature of the static and kinetic coefficients of friction, J. Appl. Phys. 22 (1951) 1373–1379.
[27] M. Barboteu, K. Bartosz, P. Kalita, A dynamic viscoelastic contact problem with normal compliance, finite penetration and nonmonotone slip rate dependent friction, Nonlinear Anal. RWA 22 (2015) 452–472.
[28] I.R. Ionescu, Q.L. Nguyen, S. Wolf, Slip-dependent friction in dynamic elasticity, Nonlinear Anal. Theory Methods Appl. 53 (2003) 375–390.
[29] S. Migórski, A. Ochal, Hemivariational inequality for viscoelastic contact problem with slip-dependent friction, Nonlinear Anal. Theory Methods Appl. 61 (2005) 135–161.